The use of LiDAR for the documentation and modelling of cultural heritage sites hidden by the forest canopy

Nikola Žižlavská*o, Stanislav Herbero

Department of Forest Management and Applied Geoinformatics, Faculty of Forestry and Wood Technology, Mendel University in Brno, Brno, Czech Republic

*Corresponding author: nikola.zizlavska@mendelu.cz

Citation: Žižlavská N., Herber S. (2025): The use of LiDAR for the documentation and modelling of cultural heritage sites hidden by the forest canopy. J. For. Sci., 71: 501–515.

Abstract: The large number of charcoal kiln sites (CHKS) preserved as cultural heritage monuments demonstrates how extensive forest management for charcoal production has influenced the present forest dynamics and contributed to industrial expansion. Therefore, it is necessary not only to have a reliable methodology for detecting and documenting individual kiln sites for management and protection purposes but also to present the results in a meaningful way to the public. The aim is to optimise the data processing workflow from airborne laser scanning (ALS) point cloud to printable model (from LAS format to STL), determine the influence of vegetation cover at the time of data collection on the quality of the resulting model, verify the quality of printed models using photogrammetry, and finally, produce printed models of CHKS as cultural heritage objects in a form that can be effectively presented to the public. After comparison of different ground filtering methods, we conclude that the most accurate method for creating a precise ground representation for our area of interest was the Cloth Simulation Filtering (CSF) algorithm. From the filtered point cloud, a high-resolution raster surface was generated, which served as the basis for CHKS detection. Using our proposed methodology – combining the topographic position index (TPI) with a 0-5% slope threshold – we achieved a significant improvement in detection performance compared to using a zero-slope threshold alone, with the F1 score increasing from 0.667 to 1.000. Subsequently, the most representative kiln site was selected, which was then processed and optimised using various software tools, resulting in an exchangeable STL file suitable for dissemination and 3D printing. The accuracy of the printable model was then evaluated. We conclude that point cloud from the winter flight campaign achieved higher accuracy. The average height differences were similar; however, the spatial distribution varied between the two clouds. The model from the winter flight campaign had more evenly distributed deviations and overall was better for modelling the CHKS.

Keywords: 3D mesh; 3D objects; 3D printing; charcoal kiln sites; photogrammetry

The cultural heritage hidden beneath the forest cover represents an important, but difficult to detect, part of the historical landscape. Limited visibility in the forested areas has long complicated archaeological research and protection of these objects. A significant advance in this area has been

Supported by the Internal Grant Agency of the Faculty of Forestry and Wood Technology, Mendel University in Brno, Czech Republic (Grant No. IGA-FFWT-22-IP-030 'Mapping abrasion phenomena using unmanned aerial vehicles and laser scanning').

[©] The authors. This work is licensed under a Creative Commons Attribution-NonCommercial 4.0 International (CC BY-NC 4.0).

brought by the availability of high-resolution digital terrain models (DTMs) acquired by airborne laser scanning (ALS). This technology has enabled the identification of small-scale anthropogenic landforms in the European landscape (Mastrolonardo et al. 2018; Tarolli et al. 2019). Combined with geographic information systems (GIS) and remote sensing (RS) techniques, ALS provides new opportunities for efficient analysis of historical landscapes that were previously possible only through time-consuming field surveys (Dell'Unto 2016). As a result, GIS has become an integral part of archaeological investigations, which, with 3D modelling technologies, expands the possibilities for spatial analysis and visualisation of the collected data (Nygren et al. 2014).

One of the important elements of the historical landscape in the forest areas of Central Europe are kiln sites - the remains of charcoal production. Production was carried out by means of charcoal kiln sites (CHKS) wooden structures covered with soil material, in which wood was burned with limited air access. This process, which dates back to the Middle Ages in the Czech lands, was crucial for the development of iron, glass, and other crafts dependent on charcoal. When charcoal production ceased, flat areas known as kiln sites were left behind. Today, these sites are crucial evidence for understanding historical forest management practices (Vinci et al. 2024). In addition to its cultural and historical significance, this method of management has also had a major impact on forest ecosystems (Ludemann et al. 2004; Bajer, Novák 2022; Lim et al. 2023). CHKS are not only evidence of former human activity, but they also represent microhabitats with distinct ecological characteristics (Schneider et al. 2020). Therefore, detecting and quantifying the distribution of individual kilns is essential for assessing the impacts of charcoal production on forest stands (Schneider et al. 2020).

However, traditional field detection of CHKS is time-consuming and often ineffective, and even in intensively surveyed areas, a high number of sites are overlooked. This fact underscores the need for the introduction of systematic approaches and the use of remote sensing technologies to enable more accurate identification and mapping of these structures. Geometric documentation is a fundamental task in the policy of protection and management of cultural heritage objects (Markiewicz et al. 2015).

Light detection and ranging (LiDAR) has become a key tool for archaeological excavations in forested areas due to its ability to penetrate vegetation cover and capture terrain relief where vegetation forms an obstacle to laser pulses. Thus, in dense forest stands, only a small number of pulses can pass through the tree canopy to the bare ground. The resulting density of points on the terrain depends not only on the flight height, scanner type and flight path spacing, but also on the species composition of the vegetation. In coniferous stands, the number of points on the ground is significantly higher during the growing season, whereas outside the growing season, due to leaf fall, deciduous stands have a significantly higher throughput (Musselman et al. 2013). As a result, LiDAR, especially ALS, plays an important role in the detection of CHKS in the forest. The dense point cloud that results from laser scanning makes it possible to detect smaller-sized landforms even under dense vegetation cover (Mokroš et al. 2021). Today, it is the most widely used technology for archaeological documentation. Other remote sensing methods used for the detection of CHKS include ground-penetrating radar (GPR), magnetometry, or electromagnetic conductivity measurement (Aspinall et al. 2008). In addition to these methods, very high-resolution imagery (VHR) is used to analyse characteristic shapes in the landscape, where CHKS leave distinctive colour variations that can be identified (Verhegghen et al. 2023).

The accuracy of detection using ALS depends on many factors, including vegetation density, technological parameters of data collection, and the visualisation methods used (slope analysis, hillshade, local relief models, etc.) (Štular et al. 2012; Schneider et al. 2020). Overall, the factors affecting the density and quality of data acquired by ALS fall into several categories technical factors (e.g. accuracy of the GPS system used, type of scanner), technological factors (flight height above terrain, flight path overlays, flight path layout), and natural factors (terrain, weather, vegetation height, growing season) (Mokroš et al. 2021). Digital documentation using LiDAR and other 3D documentation technologies is playing an increasingly vital role in cultural heritage preservation. The process begins with a laser scanner generating a dense point cloud, which captures the precise 3D spatial data of an object, such as a CHKS. This initial data structure is then

transformed into a polygonal mesh using specialised algorithms like Poisson Surface Reconstruction. This mesh serves as a detailed 3D model, essential for both digital visualisation and physical 3D printing (Ballarin et al. 2018; Comes et al. 2022).

The resulting 3D models can be exported in formats compatible with additive manufacturing, enabling the creation of tangible replicas. This capability has opened up new significant possibilities for education, conservation, and public outreach. Modern exhibitions are evolving into multi-level and multi-sensory experiences, using digital models and physical replicas to provide deeper interpretive context and engage a wider, more diverse audience (Wilson et al. 2017; Ballarin et al. 2018).

The study's main aim is to optimise the workflow for processing ALS data, from initial point cloud (LAS format) to a printable 3D model (STL format), specifically for cultural heritage sites like CHKS hidden beneath forest canopies. A key objective involves comparing various ground filtering algorithms to identify the most accurate method for generating precise ground representations of the study area. Furthermore, the research aims to develop and implement a methodology for the automatic detection of CHKS by combining LiDAR data with geomorphometric calculations and terrain classification, and to evaluate its efficacy. This includes the crucial step of selecting a representative kiln site for detailed processing and optimisation into a 3D-printable STL file, leading to the production of physical models. Finally, a significant part of the study is dedicated to assessing the accuracy and quality of these 3D-printed models using photogrammetry, while also determining how seasonal variations in vegetation cover (summer versus winter flight campaigns) during data collection influence the resulting model quality and the fidelity of the 3D prints.

This study offers valuable insights for professionals in archaeology, cultural heritage, and geoinformatics. By presenting an efficient workflow for detecting and documenting CHKS using ALS and 3D modelling, it supports more accurate identification of hidden features in forested landscapes. The approach enhances conservation efforts and opens new possibilities for education and public engagement through digital and physical representations of cultural heritage.

MATERIAL AND METHODS

Area of interest. The study area of 5 km² is located at the western edge of the Moravian Karst and the Rudice Plateau, north of the Brno city (Figure 1). The rather less rugged flat terrain is indented by very steep and deep valleys of two smaller watercourses. Evidence of the earliest settlement is linked to the High Middle Ages. There were the nuclei of two medieval villages - Klepačov and Polom, which were deserted at the beginning of the 16th century. The remains of the fields of the two original villages are preserved in similarly visible ploughlands. The area was economically linked to the exploitation and mining of iron ore, which took place in the vicinity as early as the 8th century and continued at various intervals until the 19th (20th) century.

To capture the historical significance of the region's charcoal production, a specific CHKS, highlighted in Figure 2, was chosen for precise 3D printing. This particular kiln was selected due to its representative characteristics, allowing for an accurate portrayal of the common charcoal-burning practices in the area.

Input data – ALS from winter and summer flight campaigns. The point cloud from the airborne laser scanning was taken over the University Forest Enterprise in Křtiny in winter (March) and summer (August) periods of 2024, i.e. during the non-growing and growing seasons. Scanning was performed using a Riegl LMS Q780 (RIEGL LMS, Austria) airborne laser full-waveform scanner mounted on board an aircraft (Table 1). This scanner operates at a wavelength of 1 064 nm and a maximum range of up to 5 800 m. The atmospheric conditions during the scan were favourable, with no cloud cover.

Ground filtration of point cloud. The raw point clouds from four scans were merged in R Studio (Version 4.3.1, 2023) into a single .las file. Since the raw data contains reflections of all objects on Earth, ground classification is the first step in 3D model generation. Before classification itself, noise points were removed from the point cloud using the Statistical Outlier Removal (SOR) filter (Guo et al. 2010; Lee et al. 2010; Meng et al. 2010). Identifying ground and non-ground points allows us to build a continuous terrain elevation model. During this study, we tested 3 main ground filtration algorithms available in the 'lidR' package in R.

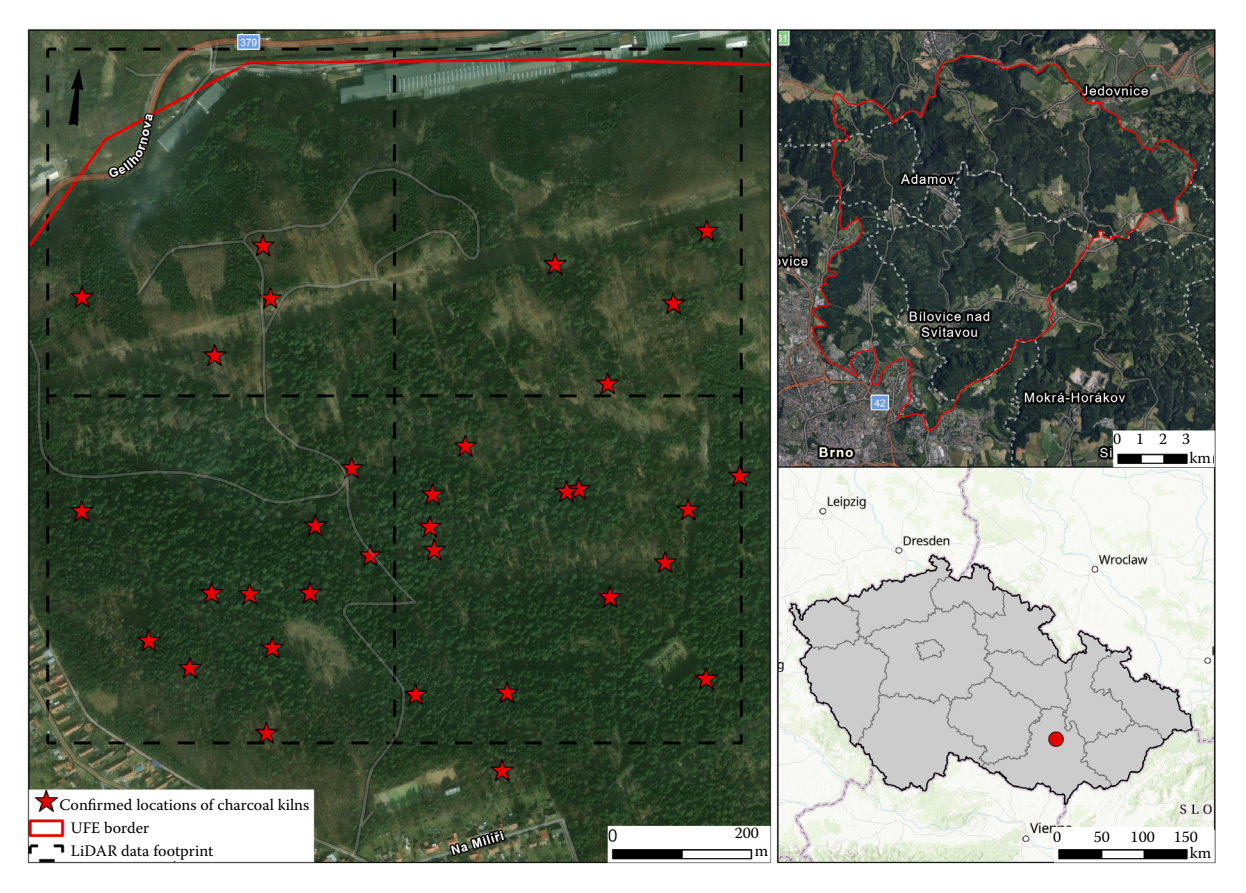


Figure 1. Area of interest showing the location of individual charcoal kiln sites (CHKS) UFE – university forest enterprise of the Mendel University in Brno

The oldest algorithm used in this study was the Progressive Morphological Filter (PMF) developed by Zhang et al. (2003). However, in the 'lidR' package, this algorithm is applied to a point layer, whereas the original method was raster-based. Another algorithm tested in this study was based on the Zhang et al. (2016) algorithm called Cloth Simulation Filtering (CSF). This method flips the input point cloud upside down and drops a virtual cloth onto the inverted surface. The ground points are then identified by examining the interactions between cloth nodes and the inverted surface. The simulation relies on a grid of particles with mass and interconnections, which collectively define the cloth's three-dimensional shape and position. Lastly, Multiscale Curvature Classification (MCC) was tested and compared. The algorithm from Evans and Hudak (2007) was originally implemented in the MCC LiDAR software (Version 2.1, 2007). We then compared each filtration method using statistical methods applied to each classified point cloud. Those methods included mean curvature, terrain roughness, surface density and variation.

Detection of charcoal kiln sites. A methodology has been developed for the automatic detection of CHKS in the field that combines the analysis of laser airborne scanning data with geomorphometric calculations and terrain classification. The first step was to create a DTM from the filtered LiDAR point cloud. This DTM served as the basis for further analysis. ArcGIS Pro software (Version 3.5.3, 2025) was used to calculate the slope of the terrain, which allowed the identification of areas with low degrees of slope. Subsequently, different indices characterising the terrain morphology were calculated in the SAGA GIS (System for Automated Geoscientific Analyses) environment (Version 9.8.1, 2021). From the Morphometry library (Version 1.0, 2001), the indices of texture, convexity, landforms, multi-resolution ridge top flatness (MRRTF), multi-resolution valley bottom flatness (MRVBF), topographic position index (TPI) and terrain ruggedness index (TRI) were tested.

The terrain slope was reclassified to extract only flat terrain portions with a slope angle of $0-5^{\circ}$, which corresponds to the expected character-

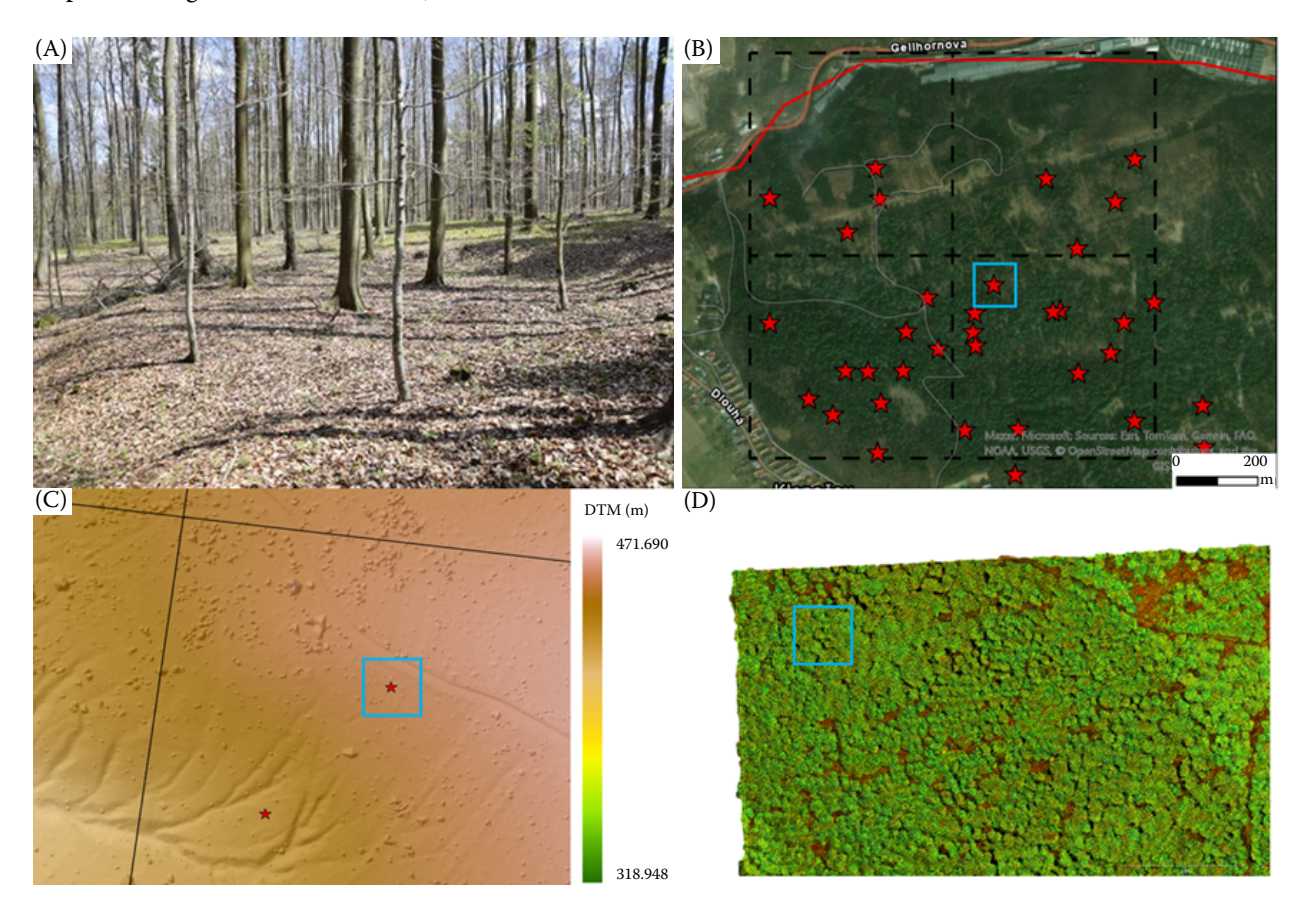


Figure 2. Selected representative CHKS used for 3D printing: (A) photo of the location in the forest, (B) the location of the study within UFE Mendelu delineated in red, (C) DTM of the location, (D) input point cloud of the location

CHKS – charcoal kiln sites; UFE Mendelu – university forest enterprise of the Mendel University in Brno; DTM – digital terrain model

istics of the CHKS. The calculated indices were then multiplied by the reclassified slope to highlight the influence of morphometric characteristics on flat areas. For manual segmentation and to verify the accuracy of the detected areas, point layer of CHKS gathered via terrain measurements was used. The field survey was conducted using a Trimble R12i GNSS device (Trimble, USA). Data collection was carried out as part of the NAKI project (Mapping the Cultural Heritage of Human Activities in Forests; ID: DG20P02OVV017). This methodology allowed for the automatic detection of potential CHKS based on their characteristic morphological features derived from LiDAR data and geomorphometric calculations.

3D printing of charcoal kiln sites. Due to the extent of the area of interest intended for the detection of CHKS and considering the limitations imposed by the 3D printing scale, one representative CHKS (terrain-verified, detected kiln sites

Table 1. Parameters of the airborne laser scanner (ALS) used in this study

Sensor	Riegl LMS Q-780			
Date of acquisition	20.03.2024, 13.08.2024			
Flight speed (m·s ⁻¹)	56			
Flying altitude (m)	1 030			
Pulse repetition frequency (kHz)	400			
Half scan angle (deg.)	600			
Spatial resolution (p⋅m ⁻²)	4			

highlighted in Figure 2) was selected for further processing. This object served as a sample for subsequent spatial analysis and physical visualisation through 3D printing. A mesh model was created for the purpose of 3D printing the CHKS model, which was processed in Meshmixer (Version 3.5.474, 2025). In the first stage, the model was loaded into this software and subjected to modifications, including extrusion in the γ -axis and sub-

sequent hole filling, resulting in a compact and printable object. Once these modifications were completed, the model was saved and exported in a suitable format. It was then imported into the PrusaSlicer software (Version 2.7.4, 2025), where the printing parameters were set. To ensure sufficient strength and quality of the model, polylactic acid (PLA) filament was used. The layer height was set to 0.15 mm, and the fill was defined with a gyroid pattern and a density of 15%. The scale and elevation were not changed. The printing parameters were also adjusted, including the number of full layers of the top and bottom of the model (3 and 3). Prior to printing, edge defects were corrected as part of the model finalisation process, and the model was cropped to a square shape, which is a common practice to optimise the final print. The G-code was then exported, and the model was printed on a Prusa MK3S+ printer (Prusa Research, Czech Republic).

Accuracy assessment of the printed model. Photogrammetric reconstruction was used to verify the accuracy of the printed model of the CHKS. The model was imaged using a digital camera with insertion points evenly distributed over its surface, which allowed for accurate georeferencing in post-processing. The images were imported into Agisoft Metashape software (Version 2.2.2, 2025), where the model was reconstructed as a point cloud.

The resulting photogrammetric cloud and the original LiDAR data were compared to quantify the geometric differences between the models. Comparisons were made between the photogrammetric model of the printed object and the LiDAR point cloud from two different flight campaigns, a summer and a winter raid. Differences in the number of points in the point cloud, including the number of areas on the surface of the model, were analysed and generated using Delaunay triangulation in CloudCompare (Version 2.13, 2023). In addition, a Cloud-to-Cloud (C2C) distance analysis was performed to measure the absolute distance of points between the compared clouds and specifically the distance of points in the z-axis, allowing the vertical accuracy of the reconstruction to be assessed. This analysis provided detailed information on the degree of agreement between the models and helped to identify potential biases arising from the 3D printing and photogrammetric reconstruction process. The main principle of the study was to create a mesh model from point cloud using different filtering techniques. This model was then 3D printed. The plastic model was then captured using photogrammetry, and new point clouds were generated. The last part was to compare each point cloud using the Cloud-to-Cloud method to establish the accuracy of the resulting model of selected CHKS (Figure 3).

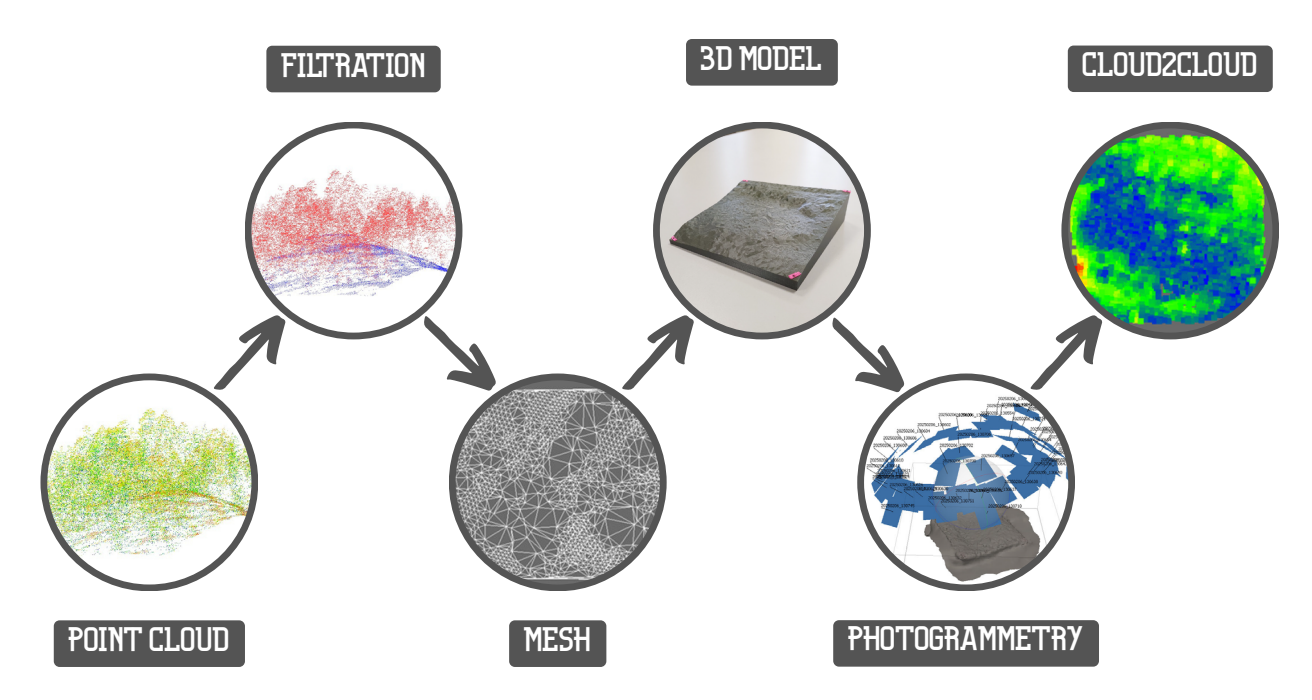


Figure 3. Flowchart of the tested methodology

RESULTS AND DISCUSSION

LiDAR point cloud density. The point density of aerial LiDAR data shows significant seasonal differences, which are primarily influenced by the phenology of the vegetation. In winter, when deciduous vegetation is without foliage, higher penetration of laser beams to the ground surface is allowed. The resulting point density at the surface averaged 0.84 points·m⁻² at this stage. In contrast, during the summer period, when the vegetation cover is fully developed, there is more scattering and absorption of the beams at the level of the tree canopy, leading to a reduction in the density of points captured on the ground (0.55 points⋅m⁻²). This difference has a major impact on the quality of the digital terrain models and the subsequent detection of subtle anthropogenic landforms. Seasonal variety is also apparent in the actual number of points of each point cloud (Table 2). Data shows that the winter dataset captured significantly more points and generated a much higher face count (number of triangles) in its mesh models compared to the summer model. If we look at a larger area with surroundings, the winter point cloud had over four times as many points, which resulted in an increased number of mesh faces.

Interestingly, for the representative CHKS, the number of mesh faces is notably higher than the number of points in both seasons. This suggests that the mesh generation process for these specific, smaller areas resulted in a high-density mesh, where multiple faces were created for each point to accurately represent the complex geometry of the kiln sites.

Models from the point cloud from the summer flight campaign. Due to the absence of reference data for quantitative evaluation of the PMF, CSF, and MCC ground classification algorithms, a visual analysis of the resulting models from the point cloud was performed. The visual inspection considered key aspects such as ground identification accuracy, smoothness of the resulting DTM, preservation of terrain details, and, most importantly, robustness to noise and outliers. The results of the visual comparison revealed differences in the behaviour of the different algorithms. The PMF algorithm (Figure 4) proved to be the least sensi-

Table 2. Differences between the number of points in point clouds and the face count (number of triangles) of generated mesh models

Point cloud	Number of points in the point cloud	Face count	
Winter flight campaign with surroundings	176 774	27 904	
Summer flight campaign with surroundings	42 626	7 216	
Representative CHKS – winter flight campaign	3 884	7 745	
Representative CHKS – summer flight campaign	1 107	2 194	

CHKS - charcoal kiln sites

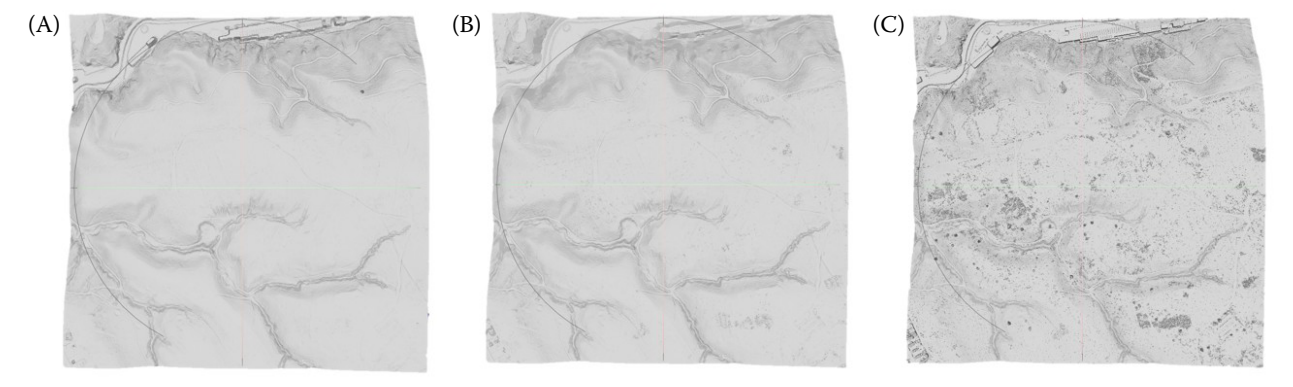


Figure 4. Comparison between resulting mesh models created from the summer flight campaign filtered with different algorithms: (A) MCC, (B) CSF, (C) PMF

MCC - Multiscale Curvature Classification; CSF - Cloth Simulation Filtering; PMF - Progressive Morphological Filter

tive to noise, but with a tendency to smooth out small terrain details. The MCC algorithm proved to be robust to noise and outliers, but with a tendency to produce artefacts in areas with complex geometry. To support these findings, we performed a statistical analysis using key metrics: mean curvature, mean roughness, surface density and surface variation. The PMF algorithm proved to be the least sensitive to noise, but this came at the cost of a tendency to over-smooth small terrain details (mean curvature = 0.808). The MCC algorithm was robust to noise and outliers; however, statistical analysis showed it often produced artefacts in areas with complex geometry, resulting in higher values for mean curvature and surface variation (mean curvature = 0.901). The CSF algorithm consistently achieved the best balance between ground identification accuracy and the preservation of terrain detail. Its statistical metrics for mean roughness and mean curvature were low enough to indicate a smooth surface, while its high surface density showed it retained a sufficient number of points to accurately represent subtle terrain features (mean curvature = 0.864). For these reasons, the CSF method was selected as the optimal approach for the subsequent detection of CHKS using geomorphometric computation methods.

The results show that the PMF algorithm was the most robust to noise but tended to over-smooth the surface. MCC handled noise well but produced artefacts in complex areas. CFS achieved the best balance of accuracy and detail preservation.

Based on the selected representative object (a single CHKS, Figure 2), spatial analyses were performed to verify its morphological characteristics and to compare the results obtained from winter and summer scanning. The results also include the evaluation of the quality of the DTM, visualisation of the kiln structure, and preparation of the

data for 3D printing. Key outputs of this analysis are presented below, including differences resulting from the use of seasonally different datasets.

Mesh surfaces. Comparison of the number of patches on the mesh surface (Figure 5A, B; Table 2) between the summer and winter flight campaigns shows significant differences in the density and distribution of triangulations. The left model (A), corresponding to the summer flight, shows a lower density of the triangular mesh, which is evident from the irregular distribution and higher variability of the plateau sizes. This effect may be due to vegetation partially obscuring the terrain and reducing the accuracy of surface detail detection. In contrast, model (B), representing the winter season, has a much denser and more regular triangulation of the network. The higher number of patches indicates better terrain coverage and more detailed surface reconstruction, which is probably due to the absence of vegetation that affects the signal backscatter in summer and thus the resulting quality of the point cloud. This difference highlights the importance of seasonality in LiDAR data acquisition, with winter flight campaigns allowing more detailed modelling of terrain structures without the interference of vegetation cover.

Detection of charcoal kiln sites. The results of the proposed methodology for detecting CHKS in the landscape are shown in Figure 6. The results show the spatial distribution of potential locations of CHKS detected using morphometric indices derived from the DTM, overlaid on the shaded relief of the region of interest. The ground truth data on the actual occurrence of kilns obtained from the field survey are marked with black dots. Detections from tested automated methods are visualised using coloured circles: MRRTF in yellow, MRVBF in orange, TPI in light blue, and TRI in dark blue. The red points represent potential false positive de-

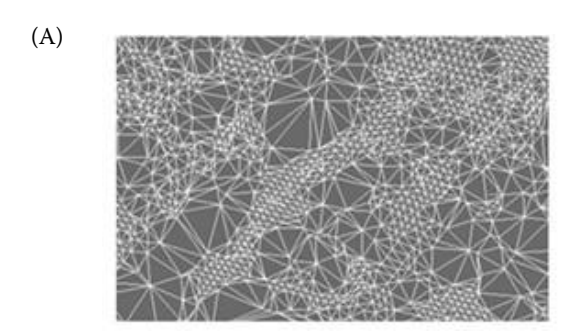




Figure 5. Comparison of face count on mesh surface: (A) summer, (B) winter

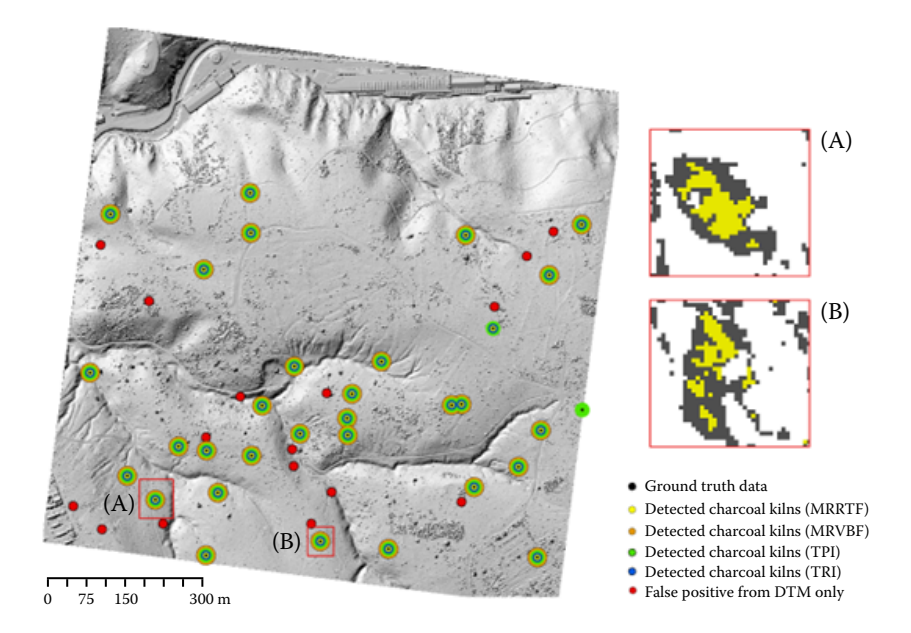


Figure 6. Detected charcoal kiln sites (CHKS) in the area of interest; (A, B) – close-up view of a detected individual CHKS MRRTF – multi-resolution ridge top flatness; MRVBF – multi-resolution valley bottom flatness; TPI – topographic position index; TRI – terrain ruggedness index; DTM – digital terrain model

tections, identified only based on DMT characteristics without application of specific morphometric indices. The analysis revealed a generally clustered distribution of potential CHKS, particularly in the central and western parts of the study area. Visual comparison of detection methods suggests differences in their spatial extent and density. The MR-RTF method appears to identify a relatively high number of potential CHKS, while the MRVBF and TPI methods show a more limited distribution of detections. The TRI method also identifies several potential sites, often overlapping with detections of other indices, primarily TPI.

The resulting raster generated by combining areas of near-zero degree slope with selected morphometric terrain indices had pixel values ranging from –26 up to 23. This composite analysis enabled the differentiation of surface features based on topographic characteristics relevant to anthropogenic modifications. Composite was then reclassified to 5 distinct classes, from which pixel values of 2 and 3 were consistently associated with locations corresponding to CHKS, indicating that these features exhibit a distinct geomorphometric signature.

The red dots, representing potential false positive detections from the analysis of DTM alone, are scattered throughout the study area, highlighting the need for additional specific approaches to refine the detection process. A more detailed as-

sessment of the spatial determination of the shape of each kiln site can be seen on the enlarged cutouts (indicated by red rectangles A and B on the main map). The dimensions of detected kiln sites A and B were compared to the dimensions measured during the terrain measurements campaign. Site A (CHKS No. 27) corresponds to a coal mining platform with an oval shape and dimensions of 14×11.5 m, dating back to the modern ages. Site B (CHKS No. 29) had dimensions of 13×10 m, with a similar shape and the same origins. The length of detected sites using our methodology was similar to measured values; however, the width was off by 2.5 m in site A, and in site B, it was again the same, but the length was off by 1 m.

The evaluation of detection was conducted using five methods by comparing the total number of detections with reference field data (this is binary information on total presence only). The methods used show slight performance differences in identifying CHKS. The absolute and percentage difference metrics showed the deviations of each method from the actual number of CHKS coming from the field survey. The recall (completeness) and precision (accuracy, assuming zero false detections) metrics and their harmonic mean F1 scores provided a more comprehensive view of performance (Table 3). The TRI method proved to be the most effective, perfectly detecting all 32 sites (recall: 1,

Table 3. Comparison of CHKS detection accuracy using different methods
--

Method	Number of detected CHKS	Field-measured data	Absolute difference	Deviation (%)	Recall	Precision	F1 score
MRVBF	30	32	2	6.250	0.938	1	0.968
TRI	32	32	0	0.000	1.000	1	1.000
TPI	31	32	1	3.125	0.969	1	0.984
MRRTF	31	32	1	3.125	0.969	1	0.984
Slope-only	16	32	16	50.000	0.500	1	0.667

CHKS – charcoal kiln sites; MRVBF – multi-resolution valley bottom flatness; TRI – terrain ruggedness index; TPI – topographic position index; MRRTF – multi-resolution ridge top flatness

precision: 1, F1: 1). Other methods, including TPI and MRRTF, showed slightly lower recall (0.96875) with perfect precision; MRVBF had lower recall (0.9375). In contrast, the 'slope only' method was notably less successful, detecting only 16 sites. This site-specific evaluation provides insight into the performance of the used methods, based on a summary of detection counts.

3D print. The results below highlight how subtle yet distinct traces of CHKS remain in the landscape. The area of the mesh model computed in Meshmixer (Figure 7) shows a naturally undulating relief typical of a forest environment, with a more pronounced terrain depression visible in the centre part of the model, which may indicate the presence of anthropogenic intervention, in this case, a relic of a CHKS.

Figure 8 displays the result of the 3D printing process, a detailed reconstruction of a specific CHKS (Figure 2). The topographical features and subtle depressions characteristic of historical CHKS are

clearly rendered, providing a tangible representation for visualisation.

Assessment of a 3D-printed model via photogrammetry. The resulting 3D model of the CHKS was assessed via a photogrammetric cloud and compared to the initial LiDAR point cloud scan of the actual terrain. Thus, not only the accuracy of the photogrammetry but also the deformations caused by the 3D printing were analysed. The comparison allowed us to analyse not only the accuracy of the photogrammetric reconstruction, but also the effect of the 3D printing itself on the geometry of the model. The LiDAR data was used as a reference model of the actual terrain, while the photogrammetry was applied to the physical 3D-printed model at a scale of 1:350. The results of the C2C analysis showed some variations (Figure 9).

Regarding the absolute distances, in the case of the summer model, the most common distances are around 25 cm. In contrast, in the winter model, these absolute distances are between 20 cm

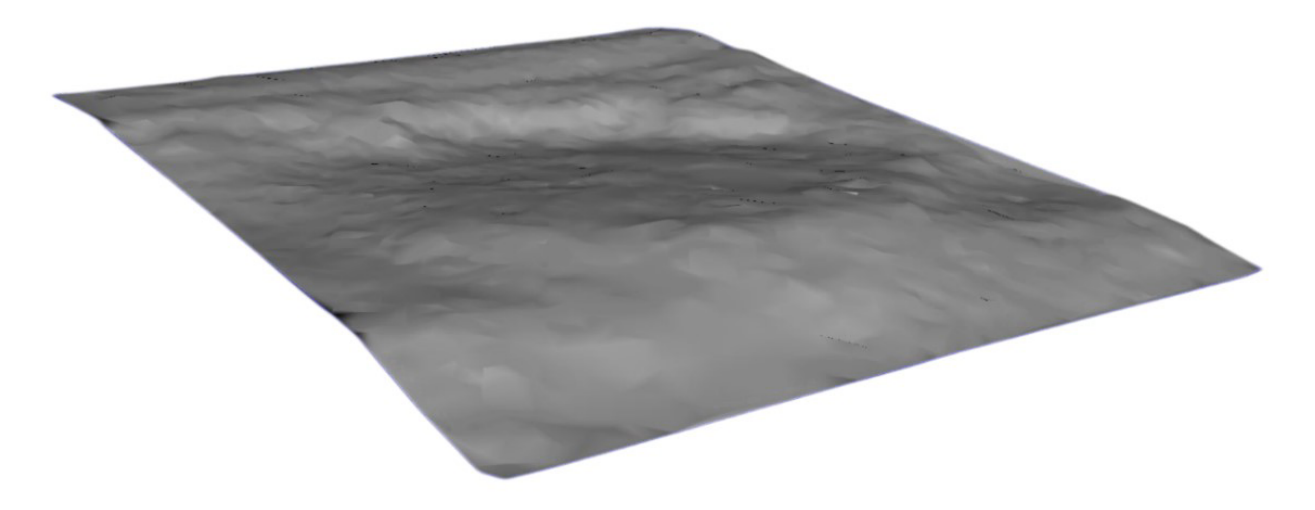


Figure 7. Generated mesh surface of a selected charcoal kiln site (CHKS) ($14 \times 11 \text{ m}$)



Figure 8. Final 3D-printed model of surface morphology of the detected charcoal kiln site (CHKS) (1:350)

and 25 cm, indicating greater accuracy. The summer model shows a distribution of deviations lower in the centre, which is the position of the flat surface of the CHKS. The average difference between absolute distances (x, y, z) of the clouds of the summer campaign is 0.47 m, whereas the average difference between absolute distances of the clouds of the winter campaign is 0.31 m. The standard deviation of the winter model is low at 0.17, so the clouds are very similar, compared to 0.28 for the summer model. The height differ-

ences (distances along the *z*-axis) are on average 0.15 m for the summer model and 0.06 m for the winter model.

The height differences are visible in the right parts of Figure 9 as well; the two point clouds are, on average, very similar. The only difference is in the spatial distribution of the deviations, with the largest differences in the upper right corner in the summer case and the deviations more evenly distributed in the winter case. However, the error in the upper right corner is there too.

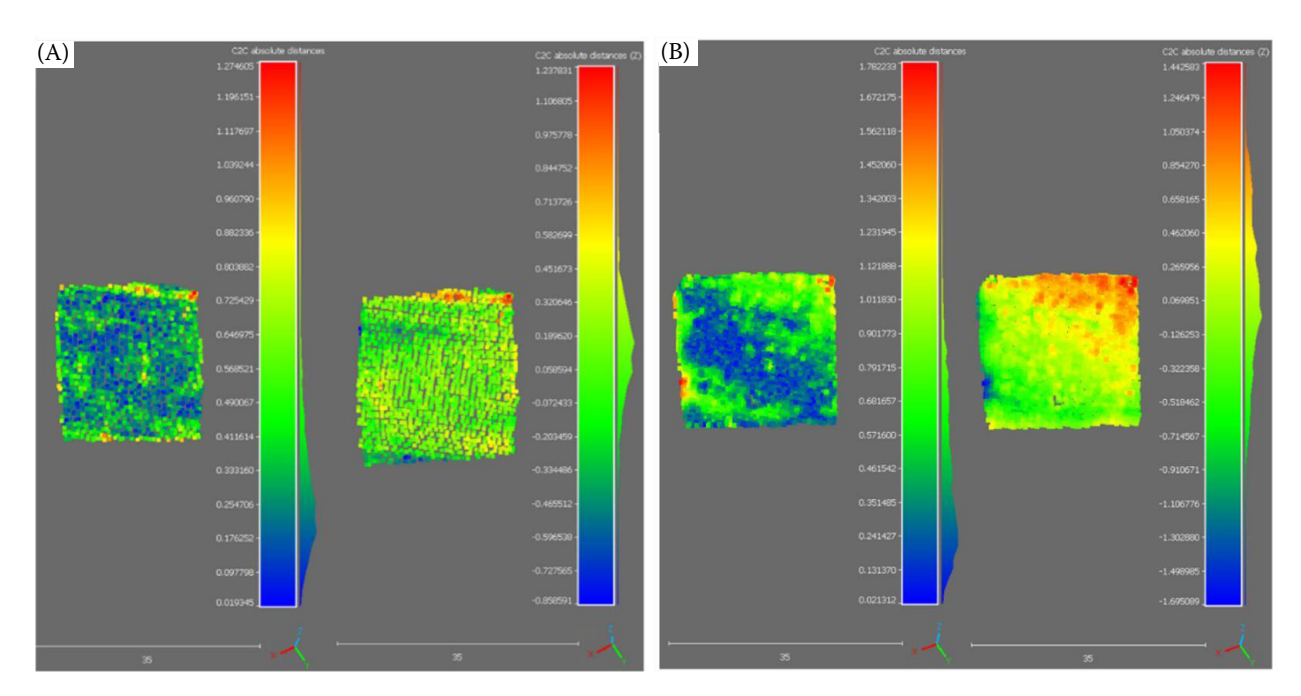


Figure 9. Comparison of point clouds from (A) summer flight campaign, and (B) winter campaign to photogrammetry point clouds of the charcoal kiln sites (CHKS)

DISCUSSION

The use of LiDAR to detect and document hidden cultural heritage structures represents a significant shift in archaeological and historical research. This technology allows us to penetrate dense forest cover and reveal terrain relics that would be difficult to identify using traditional methods. In our research, we focused on detecting CHKS from a DTM created using LiDAR and then modelled these objects using 3D printing. This study provides valuable insights into the possibilities and limitations of this method, the influence of various factors on the quality of the results, and the potential for future development.

The effects of various forestry practices can be considered an important factor affecting the legibility of terrain relics in DTM. Mechanised logging, especially the use of heavy machinery (e.g. harvesters), can lead to significant soil compaction, wrinkling of the relief, and partial or complete disruption of historical structures. On the other hand, more gentle methods of forest management, such as selective logging or manual labour, can contribute to better preservation of these sites. Repeated passage of equipment along the same routes can also have a significant impact, leading to erosion and obliteration of small microforms. However, individual CHKS are still observable in DTM despite high surface disturbances. As we have found, the preservation of historical elements can vary significantly depending on the subsequent use of the land. Intensive forestry practices can lead to erosion and damage to terrain relics, while in areas with minimal intervention, these elements can be preserved for a long time. To better understand these effects, it would be beneficial to conduct a comparative analysis using historical maps and remote sensing data. In addition, the quality of identification of CHKS is also affected by the terrain's ruggedness and shape.

When transferring these findings into physical visualisation, for instance, through 3D-printed models, additional sources of discrepancies may appear. These can result from irregularities in the layering of the 3D printing process, the effect of nozzle material and size, or interpolations in the processing of the photogrammetric data. Another factor may be the scale of the printed model, where even small inaccuracies in printing can be significant when converted to real size. The results of this

experiment highlight the importance of combining multiple techniques in digital documentation and terrain reconstruction.

Slope is an important factor influencing the presence of CHKS in the terrain. In areas with a low slope, terrain relics are less prominent, and their detection requires more sophisticated data processing methods. On the other hand, kiln sites are easier to detect on steeper slopes. It is important to further investigate which algorithms and parameters are most effective for detecting these inconspicuous objects. In addition to slope, other terrain parameters appear to be possible factors behind the presence of CHKS, including hillshade.

The presence of vegetation significantly influences the effectiveness of CHKS detection, particularly when comparing summer and winter flight campaigns using ALS. During summer (leafon) campaigns, the dense forest canopy can obscure subtle microtopographic features characteristic of CHKS, leading to reduced ground point density and potential errors in DTM generation. This can hinder the accurate identification of these archaeological features. In contrast, winter (leaf-off) campaigns are generally preferred for cultural heritage mapping in forested areas. During leaf-off conditions, LiDAR pulses can penetrate the canopy with a much higher probability, effectively reaching the forest floor. This results in a significantly denser and more accurate ground point cloud, which in turn allows for the creation of higher resolution and more precise DTMs. The improved DTM quality from winter data enables a more effective detection and detailed morphological analysis of CHKS remnants, as their subtle depressions and platforms are less obscured by vegetation. Therefore, the timing of data acquisition relative to vegetation phenology is a critical factor for successful CHKS detection and subsequent modelling (Musselman et al. 2013).

Beyond seasonal considerations, recent advancements in LiDAR technology, such as UAV-based laser scanning, offer new opportunities for improving detection of subtle archaeological features such as CHKS. UAV LiDAR allows for more flexible data collection over smaller areas with higher accuracy and potentially lower costs compared to ALS. While it may seem that higher point density automatically leads to better results, that is not always the case. For example, Kučera et al. (2023) conducted a study investigating the effect of airborne LiDAR point density on the detection rate

of historical hunting pits, which are only slightly smaller and less prominent compared to CHKS. Their analysis confirmed that detection increased from 54% to 81% when the point cloud density increased from 0.5 to 2 points·m⁻². However, when the density increased above 2 points·m⁻², there was no further improvement in detection. Furthermore, Schneider et al. (2020) used high-resolution digital elevation model (DEM) to map CHKS in their study, and found that the mapping quality varied due to heterogeneity of the DEM.

Preserving cultural heritage for future generations is one of the key tasks of archaeology, which is gaining new dimensions thanks to technological progress. Online GIS platforms represent a crucial tool for modern cultural heritage care, as they enable robust digital archiving and management by linking diverse data (maps, 3D models, documentation) with a specific geographical location, which supports long-term conservation and monitoring of monuments. At the same time, these platforms serve as a powerful tool for education and popularisation of heritage towards the general public, especially through the creation of interactive web maps, engaging visual stories [e.g. using ArcGIS Story-Maps (Paradise 2019)] and virtual 3D tours, which make cultural and archaeological wealth accessible in an attractive form and increase general awareness and interest in it (Kolte et al. 2024).

In 3D printing, it has been shown that nozzle size fundamentally affects print speed, level of detail, and mechanical properties of prints. Smaller nozzles (e.g. 0.2 mm) allow for higher detail resolution but require longer print times, which results in a higher risk of unsuccessful print completion. On the contrary, larger nozzles (e.g. 0.8 mm) speed up printing, improve layer strength, but have poorer surface quality and detail. Furthermore, the print speed can affect extrusion and error rates, especially with smaller nozzles. Nozzle temperature also has an effect, as lower temperatures can lead to poorer layer adhesion, while higher temperatures with larger nozzles improve layer bonding (Kolte et al. 2024). However, our study did not examine different materials and printers; it was only PLA material and a Prusa MK3S+ printer, so the results are affected by this and could be different for other printers. Furthermore, postprocessing (sanding, painting) was not included, which could affect the final appearance and properties of the models. For our purposes of printing at a scale of 1:350, the settings described in the methodology were sufficient (enough details, size according to the printing area).

In this research, automatic detection of milestones from a DTM created using LiDAR was used, and the objects were subsequently modelled using 3D printing. However, there is significant potential for further improvement and extension of detection methods using advanced technologies. The use of deep learning methods for automatic detection of terrain relics represents a promising direction for future research. Convolutional neural networks (CNN) can be trained on large datasets of LiDAR data and aerial imagery to identify characteristic patterns of terrain relics, while recurrent neural networks (RNN) can be used to analyse sequence data and identify terrain relics based on their spatial arrangement. Deep learning can significantly improve the accuracy and efficiency of detection, especially in challenging terrain conditions where traditional algorithms fail. In addition to deep learning, there are other advanced methods that could be used in the future, such as object-oriented image analysis (OBIA), texture analysis, and data integration from multiple sources like hyperspectral imagery, radar data, and geophysical measurements (Schmidt et al. 2016; Oliveira et al. 2021; Verhegghen et al. 2023; Guttry et al. 2025).

CONCLUSION

The use of modern technologies such as LiDAR and GIS enables systematic and accurate detection, analysis and documentation of archaeological objects hidden beneath vegetation. This study demonstrates that the combination of spatial data from both leaf-on and leaf-off seasons with advanced analytical methods opens new possibilities for archaeology and cultural heritage protection. Accurate detection of CHKS using TPI with low-slope areas from winter ALS data not only contributes to the understanding of historical management but also provides valuable insights for the conservation and sustainable management of forest ecosystems. In doing so, this approach bridges remote sensing technologies with an interdisciplinary approach to the knowledge and protection of cultural landscapes. The resulting workflow offers an efficient way to translate ALS data into tangible outcomes, supporting further research, education and public engagement in spatial modelling.

REFERENCES

- Aspinall A., Gaffney C., Schmidt A. (2008): Magnetometry for Archaeologists. Lanham, Altamira Press: 208. Available at: https://archive.org/details/magnetometryfora0000aspi (accessed Apr 3, 2025).
- Bajer A., Novák J. (2022): Cultural heritage monuments in forests, their protection and their possible use in tourism. In: Fialová J. (ed.): Public Recreation and Landscape Protection With Environment Hand in Hand... Proceedings of the 13th Conference, Křtiny, May 9–10, 2022: 74–78.
- Ballarin M., Balletti C., Vernier P. (2018): Replicas in cultural heritage: 3D printing and the museum experience. The International Archives of the Photogrammetry, Remote Sensing and Spatial Information Sciences, 42: 55–62.
- Comes R., Neamţu C.G.D., Grec C., Buna Z.L., Găzdac C., Mateescu-Suciu L. (2022): Digital reconstruction of fragmented cultural heritage assets: The case study of the Dacian embossed disk from Piatra Roșie. Applied Sciences, 12: 8131.
- Dell'Unto N. (2016): Using 3D GIS platforms to analyse and interpret the past. In: Forte M., Campana S. (eds): Digital Methods and Remote Sensing in Archaeology: Archaeology in the Age of Sensing. Cham, Springer: 305–322.
- Evans J.S., Hudak A.T. (2007): A multiscale curvature algorithm for classifying discrete return LiDAR in forested environments. IEEE Transactions on Geoscience and Remote Sensing, 45: 1029–1038.
- Guo Q., Li W., Yu H., Alvarez O. (2010): Effects of topographic variability and LiDAR sampling density on several DEM interpolation methods. Photogrammetric Engineering and Remote Sensing, 76: 701–712.
- Guttry L., Olow I.A., Paron P., Bolognesi M., Leonardi U., Stendardi L., Argenti G., Moriondo M., Dibari C. (2025): A multi-sensor remote sensing approach to monitor illegal charcoal production sites in Somalia's forests. In: EGU General Assembly 2025, Vienna, Apr 27 May 2, 2025: EGU25-17735.
- Kolte A., Bhaskaran V., Hoyle C. (2024): Optimizing 3D printing process parameters to minimize surface roughness using Bayesian optimization. In: Proceedings of the ASME 2024 International Design Engineering Technical Conferences and Computers and Information in Engineering Conference. Volume 2A: 44th Computers and Information in Engineering Conference (CIE), Washington, DC, Aug 25–28, 2024.
- Kučera A., Holík L., Knott R., Adamec Z., Volánek J., Bajer A. (2023): The soil environment of abandoned charcoal kiln platforms in a low-altitude Central European forest. Forests, 14: 29.

- Lee H., Slatton K.C., Roth B.E., Cropper W.P. (2010): Adaptive clustering of airborne LiDAR data to segment individual tree crowns in managed pine forests. International Journal of Remote Sensing, 31: 117–139.
- Lim C.K., Tan K.L., Ahmed M.F. (2023): Conservation of culture heritage tourism: A case study in Langkawi Kubang Badak remnant charcoal kilns. Sustainability, 15: 6554.
- Ludemann T., Michiels H.G., Nölken W. (2004): Spatial patterns of past wood exploitation, natural wood supply and growth conditions: Indications of natural tree species distribution by anthracological studies of charcoal-burning remains. European Journal of Forest Research, 123: 283–292.
- Markiewicz J.S., Podlasiak P., Zawieska D. (2015): Attempts to automate the process of generation of orthoimages of objects of cultural heritage. The International Archives of the Photogrammetry, Remote Sensing and Spatial Information Sciences, XL-5/W4: 393–400.
- Mastrolonardo G., Francioso O., Certini G. (2018): Relic charcoal hearth soils: A neglected carbon reservoir. Case study at Marsiliana forest, Central Italy. Geoderma, 315: 88–95.
- Meng X., Currit N., Zhao K. (2010): Ground filtering algorithms for airborne LiDAR data: A review of critical issues. Remote Sensing, 2: 833–860.
- Mokroš M., Mikita T., Singh A., Tomaštík J., Chudá J., Wężyk P., Kuželka K., Surový P., Klimánek M., Zięba-Kulawik K., Bobrowski R., Liang X. (2021): Novel low-cost mobile mapping systems for forest inventories as terrestrial laser scanning alternatives. International Journal of Applied Earth Observation and Geoinformation, 104: 102512.
- Musselman K.N., Margulis S.A., Molotch N.P. (2013): Estimation of solar direct beam transmittance of conifer canopies from airborne LiDAR. Remote Sensing of Environment, 136: 402–415.
- Nygren T., Foka A., Buckland P. (2014): The Status Quo of Digital Humanities in Sweden: Past, Present and Future of Digital History. Berlin, H-Soz-Kult: 18.
- Oliveira C., Aravecchia S., Pradalier C., Robin V., Devin S. (2021): The use of remote sensing tools for accurate charcoal kilns' inventory and distribution analysis: Comparative assessment and prospective. International Journal of Applied Earth Observation and Geoinformation, 105: 102641.
- Paradise T.R. (2019): Cultural heritage management and GIS in Petra, Jordan. ArcNews. Available at: https://www.esri.com/news/arcnews/summer12articles/cultural-heritage-management-and-gis-in-petra-jordan.html?utm_source=chatgpt.com
- Schmidt M., Mölder A., Schönfelder E., Engel F., Fortmann-Valtink W. (2016): Charcoal kiln sites, associated landscape attributes and historic forest conditions: DTM-based investigations in Hesse (Germany). Forest Ecosystems, 3: 8.

- Schneider A., Bonhage A., Raab A., Hirsch F., Raab T. (2020): Large-scale mapping of anthropogenic relief features – Legacies of past forest use in two historical charcoal production areas in Germany. Geoarchaeology, 35: 545–561.
- Štular B., Kokalj Ž., Oštir K., Nuninger L. (2012): Visualization of lidar-derived relief models for detection of archaeological features. Journal of Archaeological Science, 39: 3354–3360.
- Tarolli P., Cao W., Sofia G., Evans D., Ellis E.C. (2019): From features to fingerprints: A general diagnostic framework for anthropogenic geomorphology. Progress in Physical Geography: Earth and Environment, 43: 95–128.
- Verhegghen A., Martinez-Sanchez L., Bolognesi M., Meroni M., Rembold F., Vojnović P., Van der Velde M. (2023): Automatic detection of charcoal kilns on Very High Resolution images with a computer vision approach in Somalia. International Journal of Applied Earth Observation and Geoinformation, 125: 103524.

- Vinci G., Vanzani F., Fontana A., Campana S. (2024): LiDAR applications in archaeology: A systematic review. Archaeological Prospection, 32: 81–101.
- Wilson P.F., Stott J., Warnett J.M., Attridge A., Smith M.P., Williams M.A. (2017): Evaluation of touchable 3D-printed replicas in museums. Curator, 60: 445–465.
- Zhang K., Chen S.C., Whitman D., Shyu M.L., Yan J., Zhang C. (2003): A progressive morphological filter for removing nonground measurements from airborne LiDAR data. IEEE Transactions on Geoscience and Remote Sensing, 41: 872–882.
- Zhang W., Qi J., Wan P., Wang H., Xie D., Wang X., Yan G. (2016): An easy-to-use airborne LiDAR data filtering method based on cloth simulation. Remote Sensing, 8: 501.

Received: July 15, 2025 Accepted: September 17, 2025 Published online: October 30, 2025